



Interfacial failure mechanism in tungsten fiber reinforced copper-based composites fabricated by combustion synthesis melt infiltration under ultra-high gravity



Shibin Guo^a, Gang He^{a,b}, Guanghua Liu^{a,*}, Zengchao Yang^a, Jiangtao Li^{a,*}

^a Technical Institute of Physics and Chemistry, Chinese Academy of Sciences, Beijing 100190, China

^b University of Chinese Academy of Sciences, Beijing 100039, China

ARTICLE INFO

Article history:

Received 14 April 2015

Received in revised form 21 August 2015

Accepted 22 August 2015

Available online 29 August 2015

Keywords:

W/Cu composites

Fiber reinforced composites

Combustion synthesis

Ultra-high gravity

Fusion

ABSTRACT

Tungsten fiber reinforced copper-based composites were successfully fabricated by a new method called combustion synthesis melt infiltration under ultra-high gravity. Between the tungsten fibers and the copper matrix, an interlayer consisting of $W_{18}O_{49}$ needles was observed at the surface of the pickled tungsten fibers. The interfacial strength was measured by the push-out test. For the tungsten fibers with a WO_3 surface layer, the failure happened at the interface between the WO_3 layer and the copper matrix by the debonding failure mechanism. For the case with the formation of a $W_{18}O_{49}$ interlayer, the failure happened at the interface between the $W_{18}O_{49}$ interlayer and tungsten fibers by the brittle failure model, which improved the interfacial strength.

© 2015 Elsevier Ltd. All rights reserved.

1. Introduction

Fiber reinforced composites are usually composed of a ductile matrix and strong fibers as reinforcing agents, and an example is Cu-based composites reinforced with W fibers (briefly known as W_f/Cu) [1]. In the past 50 years, many studies have been carried out on the stress–strain behavior and the deformation mechanics of fiber reinforced metallic composites. The dependence of the elastic modulus and tensile strength of the composites on the volume fraction of W_f/Cu composites has been investigated [2,3]. Recently, W_f/Cu composites are proposed to be used for heat sink materials in fusion reactors [4–8].

In W_f/Cu composites, a stable and effective interfacial bonding between the W fibers and Cu matrix is difficult to be realized because W and Cu cannot form solid solution or intermetallic compounds. Various methods have been used to improve the interfacial bonding strength between the W fibers and Cu matrix, such as using Ni or Ti coatings and developing graded W/Cu interlayer by the PVD method [3,5]. These methods often involve complex processing and cause a degradation of the strength of W fibers.

In this work, a novel method called combustion synthesis melt infiltration under ultra-high gravity field is developed to fabricate W_f/Cu composites with improved interfacial bonding strength. This method combines highly-exothermic reactions (>2600 K) with a high-gravity

field (>1000 g, $g = 9.8 \text{ m/s}^2$) [9,10], and is effective to improve the bonding strength between the W fibers and Cu matrix.

2. Experimental

2.1. Raw materials

Commercial powders of Al (100 μm , 99.9% purity), CuO (–325 mesh, 99.9% purity), Cu (–325 mesh, 99.5% purity), black W fibers (0.5 mm, with WO_3 coating) and white W fibers (after acid pickling) were used as raw materials. The Al and CuO powders were mixed with a molar ratio of $Al/CuO = 2/3$ to prepare the thermite. The aluminothermic reaction resulted in a high temperature of 2846 K and low viscosity Cu melt was produced. Cu powder was added by 45 wt.% as diluted to make the aluminothermic reaction more stable. W fibers were cut as 15 mm short bars. Some W fibers were pickled by the mixture acid (hydrofluoric acid and nitric acid) with ultrasonic field to remove the WO_3 coating. The morphologies of the original surface and acid-pickled surface of the W fibers are shown in Fig. 1. After acid pickling, the surface of the W fibers became smooth with the WO_3 coating removed.

2.2. Materials synthesis

The reactant powders were mixed and homogenized for 1 h by rotatory ball milling with a rotation speed of 60 r/min. Each batch of 200 g mixed powders was cold-pressed into a compact with a diameter

* Corresponding authors.

E-mail addresses: lugh02@mail.ipc.ac.cn (G. Liu), lijiangtao@mail.ipc.ac.cn (J. Li).

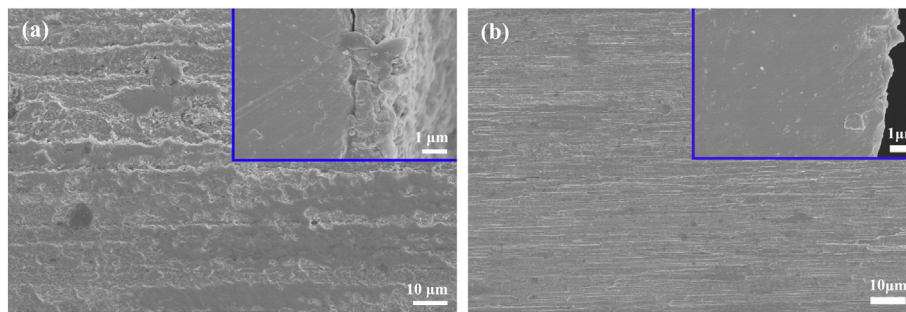


Fig. 1. SEM images of W fibers: (a) original surface, and (b) surface after acid pickling.

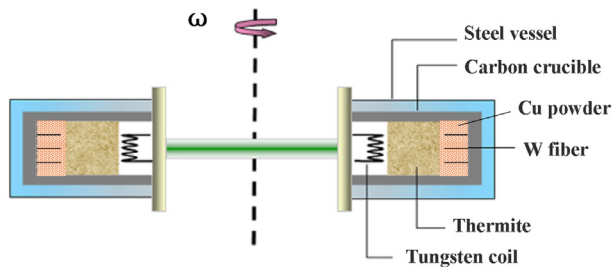


Fig. 2. A schematic illustration of the equipment for combustion synthesis melt infiltration under ultra-high gravity field.

of 40 mm and porosity about 50%. The compact was placed on a preform composed of Cu powders and 10 vol.% W fibers embedded there, which was placed in a graphite crucible. The crucible was coated with carbon felt and placed into a steel vessel, which was mounted on a rotator in a reaction chamber. The reaction chamber was evacuated to a vacuum of ~ 100 Pa. A high gravity field with an acceleration of 1000 g ($g = 9.8 \text{ m/s}^2$) was induced by the centrifugal effect. The combustion reaction was triggered by passing an electric current about 10 A through a tungsten coil closely above the reactant compact. During the reaction a large amount of heat was created, and the products of Cu and Al_2O_3 were melted. In a high gravity field, the Cu and Al_2O_3 melts were separated due to their density difference [11]. Then, the hot Cu melt rapidly infiltrated into the W–Cu preform, and after cooling and solidification W_f/Cu composite was obtained. Fig. 2 is a schematic illustration of the equipment for combustion synthesis melt infiltration under ultra-high gravity field. The as-synthesized W_f/Cu composite was machined and polished for later characterization and tests.

2.3. Characterization and tests

The interfacial bonding strength between the W fibers and Cu matrix was evaluated by the push-out tests of individual W fibers [12], using a self-made facility. The hole diameter of the supporting substrate was

3 mm and the diameter of the indenter was 0.5 mm. The loading speed was set to $8 \mu\text{m/s}$ and the displacement was about 1.0 mm. The load–displacement curve was recorded, in which the first peak indicated the onset of debonding and corresponded to a load of F_d . The interfacial bonding strength was obtained by fitting F_d with the embedded length [13]. For each sample, more than 10 tests were performed. The morphology of the interface was observed by scanning electron microscopy (SEM, S-4300, Hitachi, Japan). Elemental analysis was performed by energy dispersive spectroscopy (EDS, INCA, Oxford Instrument, UK). The crystalline phase at the interface was identified by X-ray diffraction (XRD, D8 focus, Germany) and transition electron microscopy (TEM, JEM 2100, Japan).

3. Results and discussion

3.1. Microstructure of the interface

Fig. 3 shows the microstructure of the interface between the W fibers and Cu matrix. For the W_f/Cu composite with original W fibers, the WO_3 coating bonds tightly with Cu matrix. While for the sample with acid-pickled W fibers, a new interlayer consisting of $\text{W}_{18}\text{O}_{49}$ needles is observed. Further observation of the interlayer was performed after etching Cu with FeCl_3 solution. As shown in Fig. 4, the interlayer is 2–3 μm thick and comprises fine needles with a diameter of 100–300 nm. By EDS analysis, the chemical composition of the needles are $\text{W}_{2.718-2.725}$. The XRD peaks of the needles match well with the monoclinic phase of $\text{W}_{18}\text{O}_{49}$ (JCPDS#05-0392). The strongest XRD peak can be assigned to (010) plane, implying that the needles grow along the [010] direction. From the TEM micrograph (Fig. 5(b)), the diameter of the $\text{W}_{18}\text{O}_{49}$ needle is 270 nm. The HRTEM micrograph and SAED pattern (Fig. 5(c) and (d)) reveal that the single crystal nature of the needle, and the d-spacing of 0.38 nm agrees well with the (010) plane of monoclinic $\text{W}_{18}\text{O}_{49}$. The needle-like microstructure is a typical morphology of the $\text{W}_{18}\text{O}_{49}$ phase usually formed at high temperature [14,15]. In our work, the hot Cu melt (> 1300 K) produced from the aluminothermic reaction may dissolve minor oxygen. The oxygen

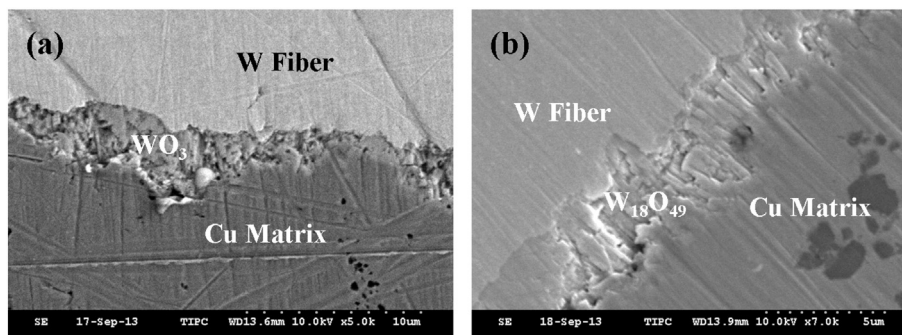


Fig. 3. SEM images of the microstructure of the interface between W fibers and Cu matrix: (a) with WO_3 coating, and (b) with $\text{W}_{18}\text{O}_{49}$ coating.

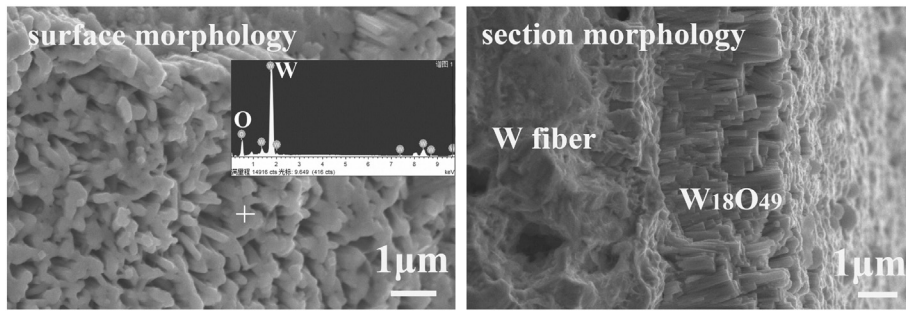


Fig. 4. SEM images of $W_{18}O_{49}$ needles after etching Cu with $FeCl_3$ solution.

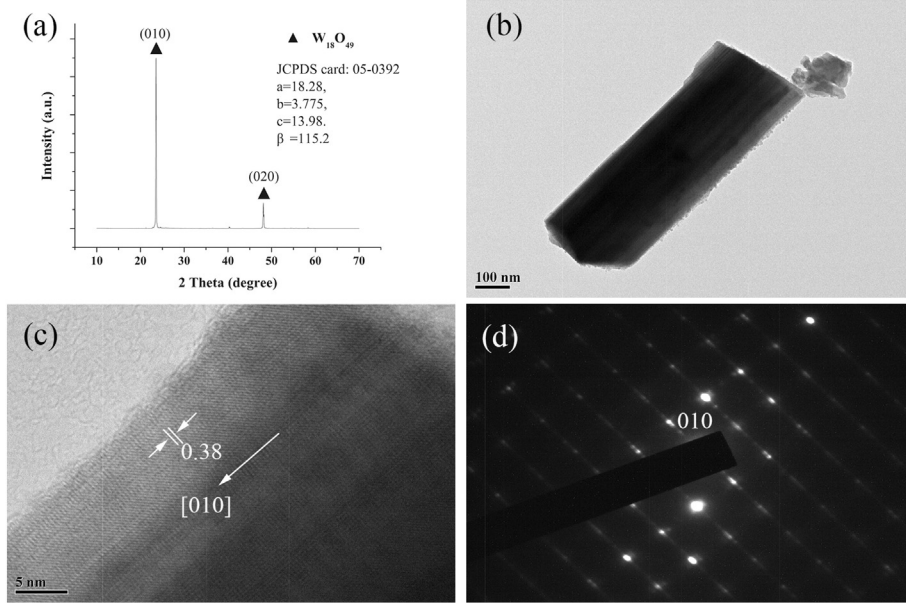


Fig. 5. Characterization of $W_{18}O_{49}$ needles: (a) XRD pattern, (b) TEM micrograph, (c) HRTEM image, and (d) SAED pattern.

atoms will react with W at the surface of the W fibers to produce needle-like $W_{18}O_{49}$ at high temperatures.

3.2. Interfacial bonding strength by push-out tests

A typical load–displacement curve during the push-out test of W_f/Cu composite is shown in Fig. 6. For the W fibers with WO_3 coating, when the linear elastic stress increases to the maximum load, interfacial

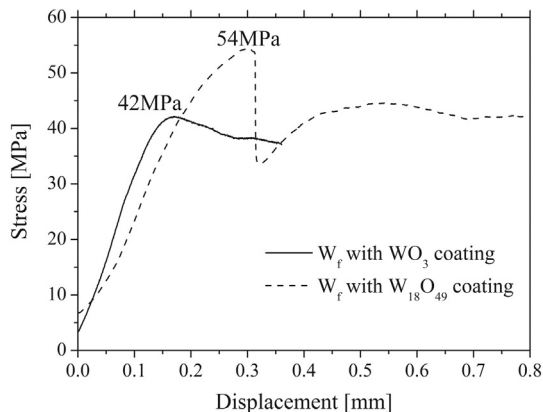


Fig. 6. A typical load–displacement curve during the push-out test of W_f/Cu composite.

debonding happens and then the W fibers bear a sliding friction stress, and the interfacial bonding strength is 42 ± 2.2 MPa. For the W fibers with $W_{18}O_{49}$ needle coating, when the linear elastic stress increases to the maximum load, interfacial brittle failure happens and the load decreases sharply and then the W fibers bear a sliding friction stress, and the interfacial bonding strength is 54 ± 3.4 MPa. The interfacial bonding strength for the sample with $W_{18}O_{49}$ needle-like interlayer is 28% higher than that of the sample with WO_3 coating, which indicates that the interfacial strength by the brittle failure model is higher than that by the debonding model in W_f/Cu composites [16].

In W_f/Cu composites, four interfacial bonding modes between W fibers and Cu matrix have been reported [5], including (1) direct interface between W fiber and the electroplated Cu matrix without deposited interlayer (interfacial strength about 20 MPa); (2) W fibers deposited with a thin Cu interlayer by magnetron sputter deposition and subsequent electroplating of the Cu matrix (interfacial strength about 25 MPa); (3) W fiber deposited with a stepwise graded transition between W fiber and the electroplated Cu matrix by magnetron sputter deposition; and (4) the same as (3) but with additional heat treatment at 800 °C. In this work, a new interfacial bonding mode is observed in W_f/Cu composites, where W fibers bond chemically with an interlayer of $W_{18}O_{49}$ needles, and contributes to an improved interfacial bonding strength.

A typical view of the specimens after push-out test is shown in Fig. 7, where the surface microstructure of the pushed fibers can be seen. Fig. 7(a) shows the rough surface of W fibers with the WO_3 coating,

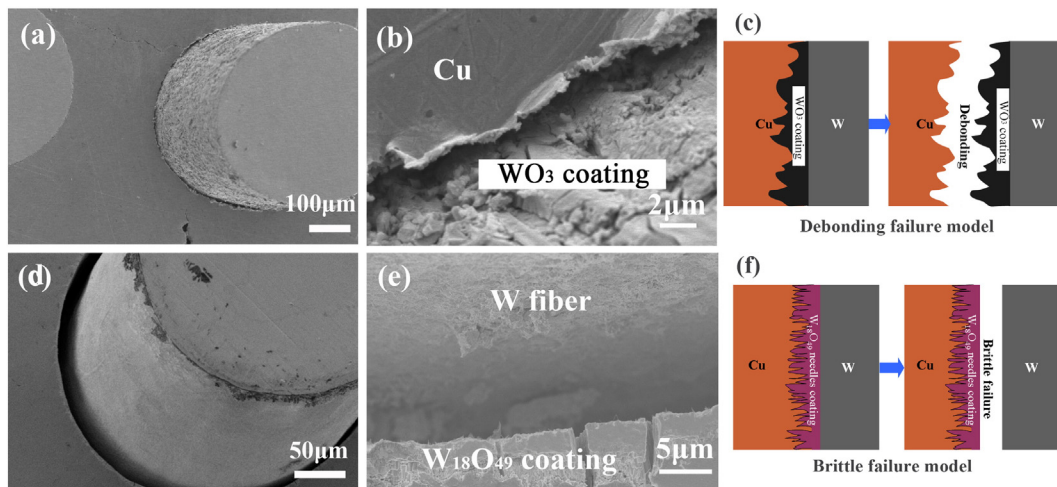


Fig. 7. SEM images of the samples after push-out tests and illustration of different failure modes: (a) rough surface and (b) debonding interface of W fibers with WO_3 coating, (c) debonding failure model, (d) smooth surface and (e) brittle failure interface of W fibers with $\text{W}_{18}\text{O}_{49}$ coating, and (f) brittle failure model.

and the failure happens at the interface between the WO_3 coating and Cu matrix by fiber/matrix debonding model. Fig. 7(d) shows the smooth surface of W fibers with $\text{W}_{18}\text{O}_{49}$ coating, and the failure happens at the interface between the $\text{W}_{18}\text{O}_{49}$ coating and W fibers by brittle failure model. There are many intergranular fracture nano-facets at the W fiber surface, which is different from the debonding model. The two failure models are simply illustrated in Fig. 7(c) and (f). The Cu matrix and interlayer are mechanically-bonded because Cu does not react with WO_3 or $\text{W}_{18}\text{O}_{49}$, and the roughness of the $\text{W}_{18}\text{O}_{49}$ interlayer with needles is larger than that of the WO_3 coating.

4. Conclusion

W fiber reinforced Cu-based composites were fabricated by combustion synthesis melt infiltration under ultra-high gravity, and the interfacial bonding strength was measured by push-out tests. A new interlayer composed of $\text{W}_{18}\text{O}_{49}$ needles was produced at the surface of acid-pickled W fibers and improved the interfacial bonding strength. For the W fibers with the WO_3 coating, the interfacial bonding strength was 42 ± 2.2 MPa, and the failure happened at the interface between the Cu matrix and WO_3 coating by the debonding model. For W fibers with $\text{W}_{18}\text{O}_{49}$ coating, the interfacial bonding strength was 54 ± 3.4 MPa, and the failure happened at the interface between $\text{W}_{18}\text{O}_{49}$ coating and W fibers by the brittle failure model.

Acknowledgments

This work is supported by National Magnetic Confinement Fusion Science Progress of China (2014GB125000, 2014GB125005), National Natural Science Foundation of China (51201173, 51422211, 51471002, 51401225), Beijing Nova Program (Z131103000413053), and Youth Innovation Promotion Association, CAS (2014024).

References

- [1] J. Karger-Kocsis, H. Mahmood, A. Pegoretti, Recent advances in fiber/matrix interphase engineering for polymer composites, *Prog. Mater. Sci.* 73 (2015) 1–43.
- [2] D.L. McDanel, R.W. Jech, J.W. Weeton, Stress–strain behavior of tungsten-fiber-reinforced copper composites, NASA Tech. Note D-1881 (1963).
- [3] D.L. McDanel, Tungsten fiber reinforced copper matrix composites, NASA Tech. Pap. 2924 (1989).
- [4] J.-H. You, Design feasibility study of a divertor component reinforced with fibrous metal matrix composite laminate, *J. Nucl. Mater.* 336 (2005) 97–109.
- [5] Herrmann, K. Schmid, H. Bolt, Interfacial optimization of tungsten fibre-reinforced copper for high-temperature heat sink material for fusion application, *J. Nucl. Mater.* 386–388 (2009) 453–456.
- [6] J.-H. You, Application of a fiber-reinforced copper matrix composite cooling tube to a water-cooled mono-block divertor component: a design study, *J. Nucl. Mater.* 386–388 (2009) 817–820.
- [7] W. Piet, M. Peters, J. Hermptenmacher, H. Schurmann, The fibre/matrix interface and its influence on mechanical and physical properties of Cu-MMC, *Combust. Sci. Technol.* 70 (2010) 1321–1329.
- [8] M. Schobel, J. Jonke, H.P. Degischer, et al., Thermal fatigue damage in monofilament reinforced copper for heat sink applications in divertor elements, *J. Nucl. Mater.* 409 (2011) 225–234.
- [9] G.H. Liu, J.T. Li, High-gravity combustion synthesis: a fast and furnace-free way for preparing bulk ceramic materials, *J. Asian Cera. Soc.* 1 (2013) 134–142.
- [10] G. He, K. Xu, S.B. Guo, et al., Preparation of tungsten fiber reinforced-tungsten/copper composite for plasma facing component, *J. Nucl. Mater.* 455 (2014) 225–228.
- [11] G.H. Liu, J.T. Li, Y.X. Chen, Phase separation in melt-casting of ceramic materials by high-gravity combustion synthesis, *Mater. Chem. Phys.* 133 (2012) 661–667.
- [12] J. Du, T. Hoschen, M. Rasinski, J.-H. You, Interfacial fracture behavior of tungsten wire/tungsten matrix composites with copper-coated interfaces, *Mater. Sci. Eng. A* 527 (2010) 1623–1629.
- [13] S. Wang, Y. Zheng, Effect of different thickness h-BN coatings on interface shear strength of quartz fiber reinforced Si O C N composite, *Appl. Surf. Sci.* 292 (2014) 867–879.
- [14] J. Pfeifer, E. Badaljan, P. Tekula-Buxbaum, et al., Growth and morphology of $\text{W}_{18}\text{O}_{49}$ crystals produced by microwave decomposition of ammonium paratungstate, *J. Cryst. Growth* 169 (1996) 727–733.
- [15] F. Liu, T. Guo, Z. Xu, et al., Controlled synthesis of patterned $\text{W}_{18}\text{O}_{49}$ nanowire vertical-arrays and improved field emission performance by in situ plasma treatment, *J. Mater. Chem. C* 1 (2013) 3217–3225.
- [16] J.W. Hutchinson, H.M. Jensen, Models of fiber debonding and pullout in brittle composites with friction, *Mech. Mater.* 9 (1990) 139–163.